IEEE Access
Multidisciplinary | Rapid Review | Open Access Journal

Received May 16, 2022, accepted June 6, 2022, date of publication June 13, 2022, date of current version June 17, 2022.

Digital Object Identifier 10.1109/ACCESS.2022.3182236

An Empirical Study of the Stochastic Nature of Electromagnetic Field Exposure in Massive MIMO Systems

FABIEN HÉLIOT[1], (Member, IEEE), TIAN HONG LOH[2], (Senior Member, IEEE), DAVID CHEADLE[2], YUNSONG GUI[2], AND MICHAEL DIEUDONNE[3]

[1]Institute for Communication Systems (ICS), 5GIC and 6GIC, University of Surrey, Guildford GU2 7XH, U.K.
[2]Department of Electromagnetic and Electrochemical Technologies, National Physical Laboratory, Teddington TW11 0LW, U.K.
[3]Keysight Technologies Belgium, 3110 Rotselaar, Belgium

Corresponding author: Fabien Héliot (f.heliot@surrey.ac.uk)

This work was supported by the European Union (EU) Project 5GRFEX entitled–'Metrology for RF Exposure from Massive MIMO 5G Base Station: Impact on 5G Network Deployment' (this project has received funding from the support for impact (SIP) programme co-financed by the participating states and from the European Union's Horizon 2020 Research and Innovation Programme), under the European Association of National Metrology Institutes (EURAMET) under Grant 18SIP02.

ABSTRACT Base stations (BSs) rely on the massive multiple-input multiple-output (mMIMO) technology in the fifth generation of mobile networks (5G). A technology having a major impact on the nature of the electromagnetic field (EMF) exposure in such systems. This work has used a fully reconfigurable mMIMO testbed (operating at 2.63 GHz), capable of mimicking realistic 5G new radio (NR) BS beamforming performance, to first gather experimental-based evidence of 5G BS EMF exposure within a real-world outdoor environment, to then analyze its stochastic behaviour, and to finally understand its impact on the definition of exclusion boundaries for 5G BSs. The exposure data of our testbed have been complemented by exposure data collected from a typical commercial 5G BS (operating at 3.65 GHz) to confirm the result trends and findings of our analysis. A robust metrology has been followed to obtain all the EMF exposure data. Our data and analysis indicate that significant exposure variations can be noticed according to the beam directions, i.e. the relative position of the exposure measurement location to the beam directions as well as the environment, confirming the stochastic nature of 5G BS exposure. The variance of the exposure tends to decrease as the number of users increase for a constant traffic load. Whereas the exposure grows sub-linearly with the traffic load, regardless of the number of users. As far as the exclusion boundary of 5G BS is concerned, its revised definition based on 95-th percentile seems still not flexible enough to accommodate the deployment of 5G BS in countries/places with stringent EMF exposure limits, as for instance in Belgium.

INDEX TERMS 5G new radio (NR), electromagnetic field (EMF) exposure, massive multiple-input multiple-output (mMIMO), experimental measurements, statistical model.

I. INTRODUCTION

The fifth generation of mobile networks (5G) is being currently rolled-out throughout the world. A roll-out that is driven by the demand for higher data rate, lower latency and higher reliability for fostering innovation and economic growth. Contrary to previous generations of mobile networks and base stations (BSs), where radio-frequency (RF) power was radiated more or less uniformly in all directions, 5G BS relies on the massive multiple-input multiple-output (mMIMO) technology. A technology capable of creating narrow directional beams for transmitting more information to different users on the same frequency/time resource, but in the process focusing more RF energy towards the specific directions of these users [1]. With new technology comes new challenges, the high directionality of mMIMO transmission, compared to previous existing cellular technologies, has raised some questions/concerns about the level of

The associate editor coordinating the review of this manuscript and approving it for publication was Wei Wei.

RF-electromagnetic field (EMF) exposure such technology can generate on the general population [2] and how to evaluate and regulate this exposure [3], [4].

The high directionality of mMIMO transmission is critical to understand the nature of the RF-EMF exposure in 5G networks. In 5G, exposure is no more considered as deterministic as with previous mobile communication technologies, but statiscal/stochastic, as it has been first suggested by the international electrotechnical commission (IEC) in [5]. Consequently, the EMF exposure metrology had to be updated for 5G BSs, with works, such as [6] or [7], proposing theoretical statistical models of the 5G BS exposure to study how its statistical aspect can impact the existing EMF regulations. Following these theoretical works, the IEC has laid the foundation in [8] for developing a practical model-based method to evaluate/extraploate the EMF exposure of in-situ 5G BSs based solely on measuring the strength of 5G BS signalling information, i.e. synchronisation signal block (SSB). Then, works, such as [9] or [10], have looked at refining this practical method by either defining a robust procedure (i.e. by mixing both classic field strength and SSB power measurements) to perform it or by considering a more comprehensive set of parameters to extrapolate the EMF exposure from the SSB measurements, respectively.

EMF Exposure from mobile equipment, e.g., BS, and mobile devices, e.g., user equipment (UE), has raised concerns about safety in the general public [2]. In response to these concerns, the International Commission on Non-Ionizing Radiation Protection (ICNIRP) [11] has provided guidelines for acceptable level of RF-EMF exposure. These guidelines are used to form regulations in many countries and regions in the world, however in an un-harmonised and often stringent manner, sometimes way below the 61 V/m recommended by the ICNIRP for the general public, e.g., 6 V/m (Italy attention value) or 9.2 V/m (new Brussels indoor limits), which can lead to BS deployment or operational difficulties [12]. In turn, these regulations are used to set exclusion boundary around BSs. Given that the nature of exposure in 5G BS is fundamentally different from previous existing BS technologies, it either requires new guidelines or a new way of defining exclusion boundary. The IEC has opted in [5] for the latter option and proposed a statistical approach to do so. The approach evaluates in a more accurate manner the actual transmit power that is radiated by a 5G BS in a realistic scenario, such that this power is defined as the 95-th percentile of the measured values instead of the theoretical maximum value. This can help to reduce the radius of the exclusion boundary of a 5G BS by 15% or 50% in comparison with the traditional deterministic approach according to [6] or [7], respectively, in turn, easing the deployment of 5G BSs.

Meanwhile, in order to evaluate the actual exposure of an operating 5G BS and understanding its impact on BS exclusion boundary, measurement campaigns have been carried out around the world. For instance, the RF-EMF exposure of 5G BSs in different test sites throughout the UK was evaluated in [13] by using an isotropic field probe with a field strength analyzer and following a procedure based on the in-situ exposure metrology set out in section B.3.1.2 of [5]. It was found that the exposure level from a typical 5G BS is only a small fraction of the ICNIRP guideline value, with the highest level recorded corresponding to only 1.5% of this value. Similar to [13], the RF-EMF exposure level of 5G BSs in different test sites throughout France was evaluated in [14]. This report concluded that the exposure of a typical 5G BS should be at worst similar to that of a current 4G BS and at best 35% lower to it. In [15], the spatial distribution of the effective isotropic radiated power (EIRP) of 25 different 5G BSs in Australia was analyzed. The analysis revealed that assuming a constant peak power transmission in a fixed beam direction leads to an unrealistic assessment of the 5G BS exposure. It also indicated that the maximum time-averaged power per beam direction is well-below the theoretical maximum EIRP, i.e. in line with the prediction of the statistical model of [7], since it leads to an exclusion boundary half the size of the one calculated by using the theoretical maximum EIRP. In [16], the RF-EMF exposure levels from different 5G services in Seoul, Korea, were measured and extrapolated based on the SSB exposure metrology approach. This study found that the time-averaged exposure was less than 5 μ W/m^2 or 1 mW/m^2 (i.e., 6 or 4 order of magnitudes below the ICNIRP limit) when exposed to a signalling beam (beam sweep) or a traffic beam of the 5G BSs, respectively. These results, even though encouraging for the deployment and operation of 5G BSs in most places, are quite disparate (1 or 3 order of magnitudes below the ICNIRP limit at full power or no traffic, respectively, in [14], and 2 or 4 order below the limit in normal operation in [13] or [16], correspondingly). This seems to indicate that the choice of metrology and parameter values in the extrapolation model are key to get consistent exposure results.

In this work, our aim is to better understand the stochastic nature of the EMF exposure in 5G BS, and its effect on the exclusion boundary definition, especially under the constraint of stringent exposure limits. Contrary to the existing works that are either theoretical [6], [7] or based solely on commercial BS [9], [13]–[15], [16], where specific beam pattern profile(s) or physical layer implementation details are unknown, i.e., a 'black box approach', we study the stochastic behaviour of exposure in 5G BS by primarily using a fully reconfigurable mMIMO testbed, i.e., a 'white box approach', which result trends are benchmarked against a classic 'black box approach'. Our testbed provides flexible evaluation of various modulation and coding schemes (MCSs), new communication algorithms and protocols as well as enabling evaluation of the relevant over-the-air (OTA) link performance. It has proved useful for measuring the spatial and temporal variations of the RF-EMF exposure in a controlled outdoor scenario to, for instance, better understand how the position of the users, number of active antenna elements, number of active beams, or number of utilized resource blocks (RBs)/ resource elements (REs) influence the exposure. Our testbed results indicate that the exposure level of a person positioned

in the general direction of an active beam can be up to nine times higher than when the beam is pointed in a different direction. They also indicate that the revised definition of the BS exclusion boundary based on 95-th percentile is still not flexible enough to accommodate the deployment of 5G BSs in countries/places with stringent EMF exposure limits. The rest of the paper unfolds as follows. Section II details our experimental setups for both the 'white box approach' and 'black box approach'. Section III then explains the calibration of our various equipment (e.g., mMIMO BS, probes) and our metrology, where both the field strength and SSB methods are used to measure the exposure. Next, the results of our measurement campaigns are provided/discussed in Section IV. We first compare the field strength against SSB results in our 'white box approach', before studying the individual effect of various parameters (e.g., UE position, traffic pattern) on the stochastic nature of the exposure in 5G BS, and subsequently its impact on the exclusion boundary definition. Conclusions are finally drawn in Section V. Preliminary versions of this work, only covering the indoor scenario, can be found in [17], [18].

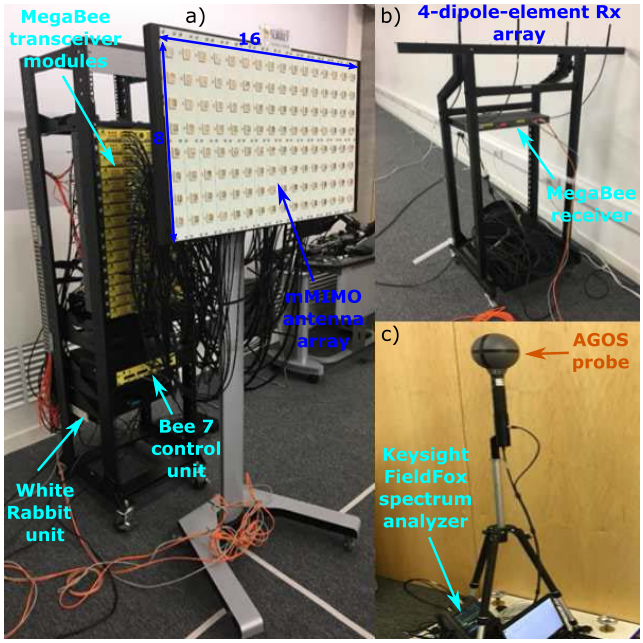

FIGURE 1. Illustration of the different elements of our mMIMO testbed: a) mMIMO BS elements; b) MIMO receivers; c) dedicated RF-EMF measurement equipment.

II. EXPERIMENTAL SETUPS

A. RECONFIGURABLE mMIMO TESTBED SETUP AND MEASUREMENT SCENARIO

Our mMIMO testbed ('white box approach') is composed of a mMIMO BS with beamforming capability for transmitting I/Q data with fully compliant 5G NR downlink waveforms, and several receivers (Rxs) as well as a probe for evaluating the RF-EMF exposure in various transmission scenarios. Its main advantage against in-situ 5G BS exposure measurement, as in [9] or [13], is its ability to independently evaluate the impact of different transmission parameters, e.g., position of the users or number of active beams, on the spatial and temporal variations of the RF-EMF exposure in controlled scenarios, e.g., line-of-sight (LoS) or non-LoS (NLoS).

The mMIMO BS of Fig. 1 a) is composed of four main elements:

1) 16 MegaBEE transceiver modules (each module comprises two parts and each part has four input/output RF ports and could support up to four I/Q channels, i.e., up to eight I/Q channels per module);
2) a BEE7 synchronization and trigger generator to control the transceiver modules and ensure that they are all synchronized with each other before transmission/reception of data;
3) a White Rabbit time distribution system for providing a reference clock signal for synchronisation to each of the transceiver module over an optical fibre link using small form-factor pluggable plus (SFP+) network adaptors;
4) a transmit antenna array with 128 (16×8) patch antenna elements mounted on a mobile stand. The array size is 0.5×0.9 m (excluding the frame) and its center stands roughly 1.8 m above the ground.

Our mMIMO BS can perform phase-coherent (after calibration) and time synchronized MIMO baseband processing by using user-programmable, reconfigurable and real-time signal processing field-programmable gate arrays (FPGAs) having software defined radio capabilities. It can simultaneously transmit data over up to 128 channels by using all of the 16 transceiver modules. It operates at a center frequency of 2.63 GHz with a bandwidth of 40 MHz, a subcarrier spacing of 15 kHz in time division duplexing (TDD), and its maximum EIRP is around 40 dBm. The 5G NR beamforming baseband signals are generated by using the Keysight PathWave System Design platform (also known as SystemVue). This software can be used to generate up to 19 potential beam directions equally spaced every 5° between $-40°$ to 50° in azimuth and 0° in elevation. Each generated beam contains a physical downlink shared channel with a configurable data payload that is transmitted within a 1-ms period. The data rate of each beam payload can be controlled by adjusting the MCS, i.e. quadrature phase-shift keying (QPSK), 16-quadrature amplitude modulation (QAM), 64-QAM, with or without channel coding, as well as the number of allocated RBs/REs used in the transmission. In our measurement campaign, the mMIMO BS used up to 96 of its 128 antennas elements to generate up to 4 beams (out of the 19 beams) for beamforming downlink data towards up to 4 active users at the same time and when considering different traffic loads, i.e., up to 216 RBs per beams. Note that up to 864 RBs in total were used for 4 simultaneously active beams and that the total transmit power of the mMIMO transmitter (Tx) system is proportional to the number of utilized RF channels. During the measurement campaign, various mMIMO downlink communication beamforming scenarios

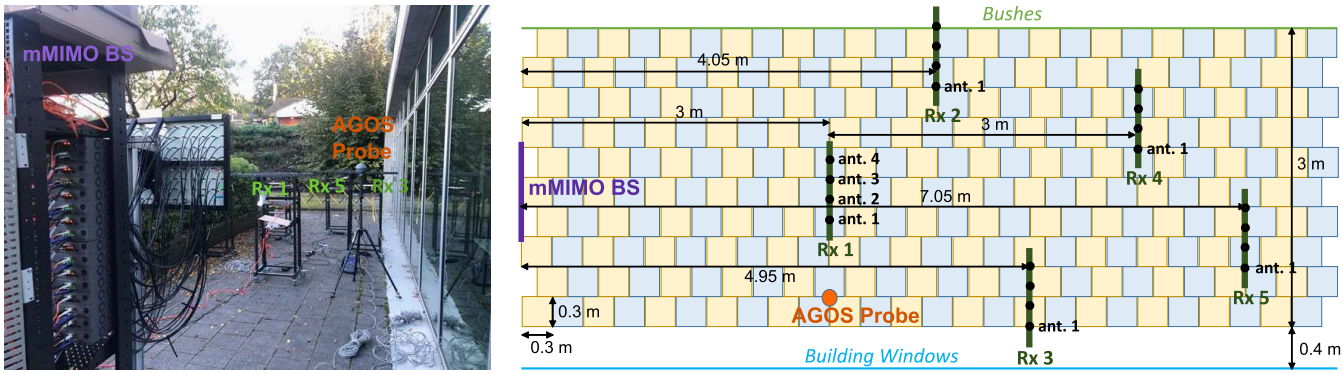

FIGURE 2. Illustration of the experimental RF-exposure measurement setup for our mMIMO testbed in an outdoor environment: a) view of the setup from the rear of the mMIMO BS; b) detailed layout of the setup showing the positions of the various utilized equipment.

were considered, with different combinations of active beams and traffic data loads to mimic a realistic 5G BS operation.

Our testbed uses several receivers, as it is shown in Fig. 2 a). The receivers can either be used as probes to measure the amplitude of the received signal at a given spatial location or to mimic MIMO UEs. They each comprise one MegaBEE transceiver module, which provides up to eight output RF ports, for performing the MIMO baseband processing, as it is illustrated in Fig. 1 b). The RF ports are connected to up to eight vertically polarized dipole antenna elements mounted on a mobile trolley.

Our testbed also includes a dedicated RF-EMF measurement system (in addition of the receivers that can also be used for this purpose) that is composed of an AGOS SDIA-6000 triaxial isotropic field probe (placed on a tripod) and an handheld Keysight FieldFox N9917B portable spectrum analyser [19], as it is depicted in Fig. 1 c). The probe can measure both the electric-field (E-field) or magnetic field (H-field) strength. It consists of three isotropic mutually orthogonal sensors, which can simultaneously measure the exposure over the x-, y- and z-axes and provide a vector sum of the field magnitude, independent of the polarization or direction of propagation of the electromagnetic wave.

Our testbed was placed in the outdoor patio area of the 6G Innovation centre building at the University of Surrey in Guildford, UK (51°14'36.1″N 0°35'34.2″W), as it is shown in Fig. 2 a). The detailed layout and precise locations of the various equipment of our testbed are provided in Fig. 2 b).

B. COMMERCIAL 5G BS SETUP AND MEASUREMENT SCENARIO

The 'black box approach' provides a realistic in-situ evaluation, in a classic outdoor environment, of the exposure of a typical commercial 5G BS. During the measurement campaign various varying factors such as the number of users, position of users and targeted data rate of users were considered. The measurement campaign took place at the BT's trial field site, within the BT's Adastral Park, in Ipswich, UK (52°03'28.1″N 1°16'44.5″E), as it is depicted in Fig. 3.

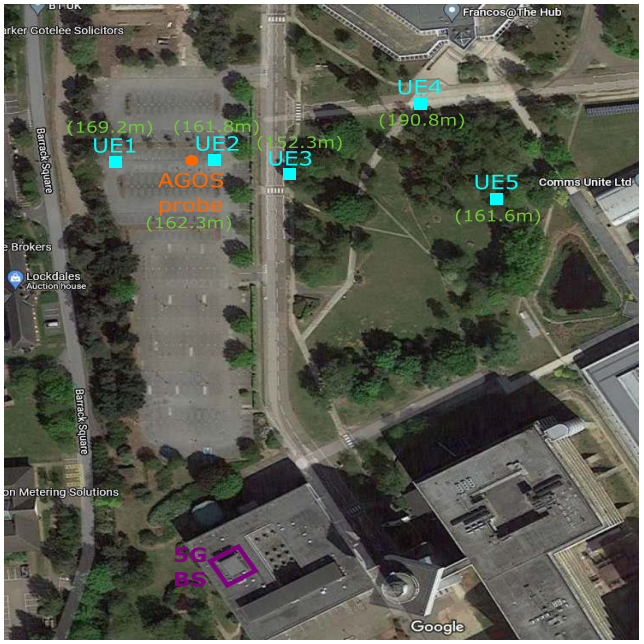

FIGURE 3. Aerial view of the experimental RF-exposure measurement setup for the commercial 5G BS at the BT's Adastral Park showing the positions of the various utilized equipment.

One typical 5G BS, provided by Samsung, was utilized for the campaign, while all the other 4G and 5G BSs present on the site were turned off to avoid potential interferences. The 5G BS operates in TDD mode over the 3.5 GHz (n78) 5G NR frequency band with a bandwidth of 100 MHz. Its mMIMO unit comprises 32 transmit and 32 receive RF chains for a total of 96 antenna elements that are split in four vertical sub-arrays having three rows of eight cross-polarised elements, a.k.a, 4V8H configuration. The RF output power of the BS is 80 W, while its EIRP is around 71 dBm. More details about the 5G BS configuration and capability can be found in [20]. The 5G BS was located at the top of a multi-storey building (at a height of 20 m above the ground level) in the southern part of the test campaign area (i.e., in the lower part of Fig. 3). The test site included a car park and a grassland area with trees.

FIGURE 4. Ground view of the various equipment used in our exposure measurement setup for the commercial 5G BS: a) Samsung 5G mobile phone (UE3) with 'iPerf' application; b) view of the test site and 5G BS location from the rear of UE1 (mounted on a tripod); c) view of the test site from the left side of the AGOS probe, showing the AGOS probe and UE2 relative position; c) view of the test site from the rear of UE5.

A double-storey building (i.e., a restaurant) lies at the back of the grassland area (north of UE4 location in Fig. 3).

In addition to the 5G BS, five Samsung 5G mobile phones/UEs, most of them mounted on tripods, were utilized as test terminals (see a close-up of one of them in Fig. 4 a)), referred to as UE1 to UE5 in Fig 3. They were used for initiating downlink data transmission and were distributed in five different fixed locations around the test site. Their specific locations and corresponding distances to the 5G BS is reported in Fig. 3. Their locations were chosen to include both LoS (e.g., UE2 was placed in an open area, see Fig. 4 c)) and NLoS (e.g., UE5 was placed behind trees, see Fig. 4 d)) scenarios. The 'iPerf' application (see Fig. 4 a)) was used by each UE terminal for initiating the connection with the 5G BS. Different data rates could be configured by setting appropriate parameters in the main script. The targeted data rate of each UE was set between 30 Mbps, e.g., for five active UEs simultaneously requiring a low data rate, to 700 Mbps, e.g., for a single active UE requiring a high data rate. Whereas the AGOS probe (see Fig. 4 c)) was employed for measuring the RF-EMF exposure. The probe was placed in an open area near UE2 that was in LoS with the BS. As with the UEs, the probe position was fixed during the whole measurement campaign.

III. RF EXPOSURE MEASUREMENT CALIBRATION AND METHODOLOGY

In order to ensure the traceability of our results, the various equipment used in our two experiments of Section II were first calibrated prior to any RF-EMF exposure measurement, as it is further detailed in the following. Besides, two different approaches for measuring the exposure were utilized in our work: a classic one based on measuring the E-field strength at different locations by using dedicated exposure equipment (e.g., probe), and a simplified one that extrapolates the exposure based on the received signal reference power (RSRP) at the UE. The idea here being to establish if the RF-EMF exposure of 5G BS can accurately be evaluated based solely on the signaling part of the transmit signal.

A. CALIBRATION AND TRACEABLE RF-EMF MEASUREMENT

On the one hand, the dedicated RF-EMF measurement system (Keysight spectrum analyser and AGOS probe) was calibrated at the UK National Physical Laboratory (NPL) in its power flux density laboratory against known generated E-field. Whereas each component of the receivers, i.e. MegaBEE modules, dipoles antennas, and cables were first calibrated separately. For instance, the MegaBEE modules were calibrated to test their sensitivity to RF received power by using power sensors, while the dipole antennas were calibrated by using the three antenna method [21].

On the other hand, the mMIMO BS was calibrated in situ (at the same physical location of the experiment) by relying on an OTA-based multi-channel transmitter calibration method. Given the inherent uncertainty of phase and delay caused by multiple RF channels, multi-channel calibration is a crucial factor affecting the beamforming performance of typical mMIMO antenna arrays. Even though the accuracy of the multi-channel calibration method is higher in an anechoic chamber, it is still quite effective in a multi-path environment when verified by experimental measurements [22], [23]. In addition, this calibration method does not require any extra hardware circuits to simultaneously obtain the RF calibration factors of multiple channels, which makes it easier to perform in-situ with heavy and cumbersome equipment like our mMIMO BS.

1) OVER-THE-AIR CALIBRATION FOR mMIMO BS

Our OTA-based calibration method uses a multi-antenna pilot scheme based on frequency division multiplexing (FDM) that simultaneously transmit 10 antenna pilot signals (equally spaced in the frequency domain) for each orthogonal FDM (OFDM) symbol. By using enough OFDM symbol REs, it can provide a reliable pilot pattern for very large numbers of active transmit antennas. At the receiver, the channel for each transmit antenna is estimated based on the pilot signals, where the LoS component of the received signal transmitted over the i-th row j-th column element of the mMIMO BS array is usually modeled as

$$y_{i,j}^{\mathrm{LoS}}(t) = s(t-\tau_{i,j})\alpha_{i,j}\beta_{i,j}\exp(j(\phi_{i,j}+\theta_{i,j})). \quad (1)$$

In (1), $s(t)$ is the ideal transmit waveform (without impairments), and $\tau_{i,j}$, $\alpha_{i,j}$, as well as $\phi_{i,j}$ model the delay, amplitude, as well as phase impairments of the i-th row j-th column element of the mMIMO BS array, respectively. Besides, $\beta_{i,j}$

and $\theta_{i,j}$ represent the amplitude and phase variations of the LoS path. Note that $i \in \{1, 2, \ldots, 16\}$ and $j \in \{1, 2, \ldots, 8\}$ for our array. The OTA process for calibrating our mMIMO includes three main stages:

1) The time domain channel impulse response (CIR) is first acquired based on the estimated frequency-domain channel response.
2) The multiple paths of the channel are then separated and $\tau_{i,j}$ is estimated to compensate for them. In an ideal environment such as a microwave anechoic chamber, estimations of the time delay, $\tau_{i,j}$, the combined amplitude, $\alpha_{i,j}\beta_{i,j}$, and the aggregated phase, $\phi_{i,j}+\theta_{i,j}$, of the direct LoS path can be easily obtained based on the CIR. Whereas in the multi-path scenario, it is necessary to consider the impacts of the parameter estimation accuracy such that a signal separation algorithm for multi-paths overlapped CIRs, based on the maximum likelihood criterion, needs to be utilized to estimate these parameters.
3) Finally, $\phi_{i,j}$ is estimated and removed from the transmit signal to ensure that the array steers its beam in the desired direction. Indeed, it is important to note that the phase of the LoS path for the i-th row j-th column antenna element depends on the relative position of the transmit array towards the receiver such that $\theta_{i,j}$ can be expressed as

$$\theta_{i,j} = \theta_{\text{ref}} + \Delta\theta_{i,j}^{a,b}, \tag{2}$$

where θ_{ref} is the phase of the LoS path between the a-th row b-th column element of the array and the receiver and $\Delta\theta_{i,j}^{a,b}$ is the i-th row j-th column component of a steering matrix, which assumes the element (a, b) of the array to be the reference element. The phase difference $\Delta\theta_{i,j}^{a,b}$ reflects the fact that each antenna element has a slightly different position relative to the receiver. Given that $\Delta\theta_{i,j}^{a,b}$ is inherent to the array, its knowledge can be easily acquired such that its effect can be removed from the aggregate phase, i.e., $\phi_{i,j}+\theta_{i,j}-\Delta\theta_{i,j}^{a,b} = \phi_{i,j}+\theta_{\text{ref}}$. Next, the relative phase between all the elements of the array can easily be obtained by subtracting the residual phase of element (i, j), i.e. $\phi_{i,j}+\theta_{\text{ref}}$, from other element residual phases, such that any phase misalignments can be corrected at the transmitter.

Figure 5 depicts the results of an example of time and phase compensations when using our OTA calibration method for our mMIMO BS. More specifically, Figs. 5 a) and b) show the LoS path time delay and phase difference before and after the calibration, respectively, for the 16 antenna elements of the fifth row of our mMIMO array of Fig. 1, when considering 10 different channel realisations (indicated by different color on the figures). It is clear from Fig. 5 b) that the phase and timing differences across most of antenna elements are adequately compensated, i.e. all the delay values are very similar and most of the phase values are very close to 0 radian, after applying our OTA calibration method to the multiple RF

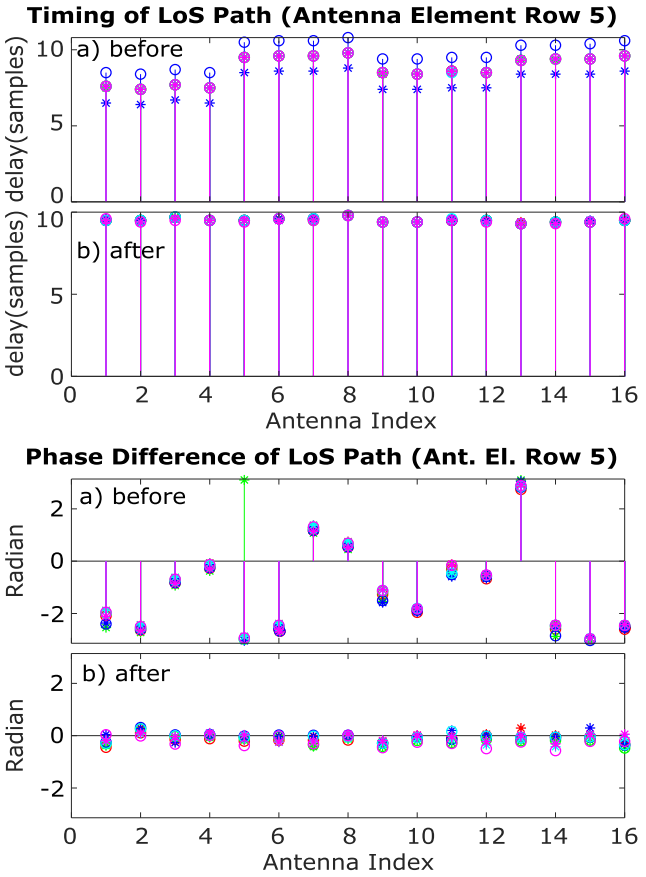

FIGURE 5. LoS path time delay and phase difference: a) before and b) after the OTA calibration process for the 16 antenna elements of the fifth row of our mMIMO antenna array.

channels. In turn, this demonstrates the effectiveness of our mMIMO BS calibration procedure.

2) TRACEABLE MEASUREMENT WITH A FIELD STRENGTH PROBE

Field strength probes are often used to measure the E-field or H-field strength. In practice, the characterization of a field strength usually only requires the measurement of either its E-field or H-field. A field strength probe is not designed to be calculable but its calibration require to set up a known EMF defined by parameters that can be readily made traceable to national standards. These parameters are the power, impedance, attenuation and length. The probe sensitivity (normally reported as a correction factor in terms of the measured and true 'known' field) along the x-, y-, or z-axis can be measured separately by aligning each sensor of the probe in turn with the calibrating field inclined at an angle of 54.7° to its handle, i.e., one of the axes is positioned perpendicular in the generated field every 120°. After calibration, the RF-EMF exposure can be calculated as

$$\varepsilon = \sqrt{(E_x\delta_x)^2 + \left(E_y\delta_y\right)^2 + (E_z\delta_z)^2}, \tag{3}$$

when using a field strength probe. In (3), E_i represents the i-axis E-field measured by the probe, δ_i is the i-axis correction factor resulting from the independent calibration process of

each axis. Meanwhile, the i-axis E-field is proportional to the square root of the channel power at a distance d from the E-field source, i.e.

$$E_i = \sqrt{\eta_0 \gamma_i(d)}, \tag{4}$$

where $\eta_0 = 120\pi\ \Omega$ is the wave impedance of a plane wave in free space and $\gamma_i(d)$ is the i-axis channel power measured at a probe placed at a distance d from the E-field source. Hence, by inserting equation (4) into (3), the measured RF-EMF exposure at a probe can then be re-expressed as

$$\varepsilon = \sqrt{\eta_0 \left(\gamma_x(d)\delta_x^2 + \gamma_y(d)\delta_y^2 + \gamma_z(d)\delta_z^2\right)}. \tag{5}$$

Note that in theory, $\gamma_i(d)$ is given by

$$\gamma_i(d) = \frac{P_i G_i}{4\pi d^2}, \tag{6}$$

where P_i and G_i are the i-axis transmit power and antenna gain of the E-field source, respectively, and $4\pi d^2$ represents the surface of a sphere of radius d.

3) TRACEABLE MEASUREMENT WITH MULTI-ANTENNA RECEIVERS

As already previously mentioned, the multi-antenna receivers mounted on trolleys can also be used to measure the RF-EMF exposure. This is done by converting the amplitude of the received signal at each of the receiver antenna into exposure information via the following equation

$$\varepsilon = V C_{\mathrm{L}} A_{\mathrm{F}} C_{\mathrm{AG}}, \tag{7}$$

where V is the received signal voltage measured at each antenna of the receiver, C_{L} accounts for the cable loss, A_{F} is the antenna factor to account for the field in the air, such that $A_{\mathrm{F}} = E/V$, with E being the plane wave E-field. In addition, C_{AG} is the corrective factor that accounts for the automatic gain control that is implemented in each MegaBee transceiver module. The values of C_{L}, A_{F}, and C_{AG} have been obtained through calibration and validated by ensuring that the EMF values obtained by each antenna of each receiver well-match EMF theoretical values as well as values obtained with the AGOS probe and a calibrated commercial Narda probe (i.e. a Narda NBM-550 meter with a Narda EF-0392 probe).

Figure 6 shows the result of the validation process, after calibration, for the four dipole antennas of receiver Rx 1 in Fig. 2 a). It is clear from the results that the E-field values measured via the four antenna elements of Rx 1 are inline with the theoretical and probe measured values, especially at low transmit power, and that they well match each other.

B. E-FIELD STRENGTH VS. SSB-BASED RF-EMF EXPOSURE MEASUREMENT METHODS

Two different methods have been followed in our work to measure the EMF RF-exposure, i.e., either the traditional E-field strength approach or the SSB approach.

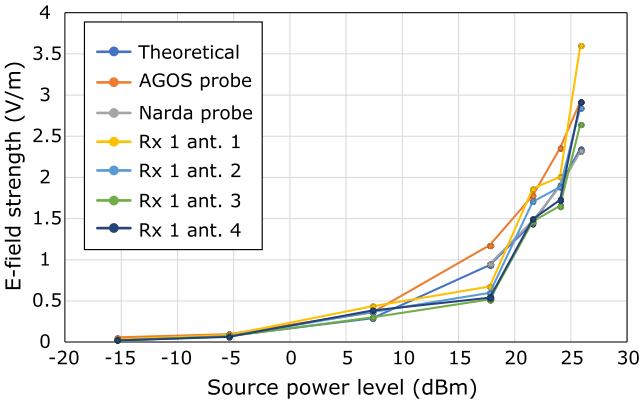

FIGURE 6. Comparison of the theoretical E-field with the measured E-field of two different probes (AGOS and Narda) and the four antennas of Rx 1.

1) E-FIELD STRENGTH MEASUREMENT METHOD

In this method, we used the AGOS probe plus five multi-antenna receivers (having four antennas each) in the mMIMO testbed setup or the probe on its own in the commercial 5G BS setup, as it is depicted in Fig. 2 or Fig. 4, correspondingly, for measuring the raw E-field/received signal power over the whole transmission bandwidth. The signal power depends on the short term channel configuration, e.g. MCS, RB/RE allocation, at one or different geographical locations. For the mMIMO testbed, the multi-antenna receivers were used as extra probes such that the received RF power was measured at 21 different locations for each transmit signal, whilst the mMIMO BS was not necessarily transmitting/steering a beam towards the receivers or AGOS probe; this allowed us to acquire more measurements and get a better statistical view of the RF-EMF exposure. In both setups, the E-field values were captured by the probe and then converted into exposure data via (5). In addition, for the mMIMO testbed, the received signal amplitude values were captured by the receivers and then converted into exposure data via (7). The height of the AGOS probe and receiver antennas was around 1.5 m from the ground.

2) SSB-BASED MEASUREMENT METHOD

The idea being the SSB-based RF-EMF exposure measurement method for 5G BS, which has already been well-discussed in the literature [8]–[10], [16], is to extrapolate the exposure based on the RSRP, which is itself obtained through synchronization signals. In a 5G system, the SSB consists of a block of 240 subcarriers and 4 OFDM symbols containing the primary synchronisation signal (PSS), the secondary synchronisation signal (SSS), the physical broadcast channel (PBCH) and the PBCH demodulation reference signal (PBCH DM-RS) [24]. The SSBs are usually grouped in block patterns called synchronization signal bursts. Contrary to the E-field strength method, which measures the raw received signal power for a specific frequency bandwidth and time window regardless of the RF signal sources, the SSB-based method extrapolates the RF signal power by first extracting the SSS from the received signal (with the aid of a

unique scrambling sequence for each BS) and by then obtaining the RSRP. Next, the RF-EMF exposure is extrapolated from the measured RSRP for each RE, such that a generic definition of the maximum E-field strength can be formulated as [9]

$$E_{\max} = E_{\mathrm{SSB}}\sqrt{F_{\mathrm{ExtSSB}}}, \tag{8}$$

where E_{SSB} is the field level (V/m) per RE of the SSB and F_{ExtSSB} is the extrapolation factor of the SSB. More specifically, F_{ExtSSB} can be decomposed as

$$F_{\mathrm{ExtSSB}} = F_{\mathrm{ExtBeam}}F_{\mathrm{BW}}F_{\mathrm{TDC}}F_{\mathrm{PR}}, \tag{9}$$

according to IEC 62232 F.9.2.1.4. In (9), F_{ExtBeam} is the extrapolation factor corresponding to the ratio of the EIRP envelope of all traffic beams to the EIRP envelope of the broadcast signal at the direction of the measurement location, F_{BW} is the total number of subcarriers within the carrier bandwidth, F_{TDC} is the technology duty cycle, i.e., the ratio between the total number of occupied REs and the total number of REs in one synchronisation signal burst period, F_{BW} is the total number of subcarriers within the carrier bandwidth, and F_{PR} is the ratio between the actual maximum average data rate (of the experiment) and the theoretical maximum data rate.

In order to implement this method, we used the AGOS probe, i.e., acting as a UE, to extract the SSS from the BS received signal (by using the BS unique scrambling sequence) and obtain the RSRP. The RF exposure was then extrapolated from the RSRP by using equations (8) and (9).

IV. RF-EMF EXPOSURE MEASUREMENT CAMPAIGN AND DISCUSSIONS

Given the statistical nature of the RF-EMF exposure in 5G networks, it is expected that the exposure of a person located within the coverage area of a 5G BS but not necessarily using their UE, i.e., a bystander, would be affected by various factors; one of them being the relative position of active UEs in their vicinity, given that active UEs trigger the generation of an E-field from the BS. In addition, the number of active UEs, the data traffic pattern of these UEs, and/or environmental fluctuations can also impact the bystander exposure. Accordingly, we have used both our measurement campaigns with the mMIMO testbed and commercial 5G BS to analyze the impact of such factors on the exposure and the definition of the exclusion boundary for 5G BS. We have also used our mMIMO system to test the accuracy of the SSB-based method of Section III-B2 in comparison with the classic E-field strength measurement method of Section III-B1.

Note that, after calibrating all the equipment, tens of thousands of E-field/receive amplitude measurements (i.e., measurements were taken over a 48h period and each measurement lasted 50 seconds for the 21 locations) were acquired by the AGOS probe and multi-antenna receivers for determining the RF-EMF exposure through both the E-field strength and SSB-based methods in the mMIMO testbed measurement campaign. Whereas hundreds of E-field measurements

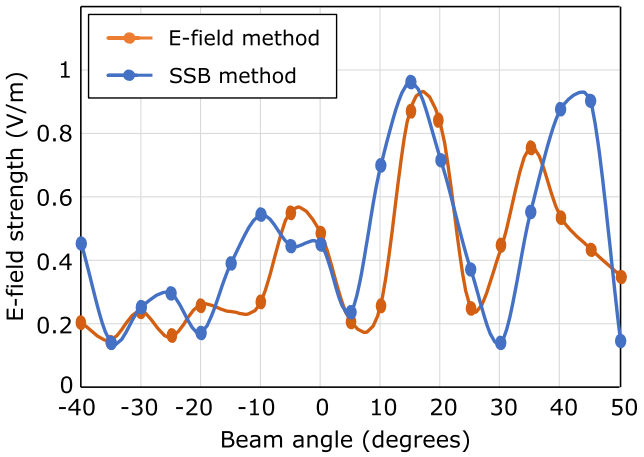

FIGURE 7. RF-EMF exposure distribution comparison between the E-field strength measurement and SSB-based extrapolation methods for the mMIMO testbed with 96 active antennas.

(i.e., measurements were taken over a 48h period and each measurement lasted 6 mins) were acquired by the probe for determining the exposure through the E-field strength method in the commercial 5G BS campaign. The noise floor level for both the mMIMO testbed and commercial BS measurements was close to -90 dBm.

A. SSB-BASED METHOD ACCURACY VALIDATION

In order to evaluate the accuracy of the SSB-based method in comparison with the E-field strength method, we first provide a comparison of their results in Fig. 7 when using the mMIMO tested with 96 active antennas. In the SSB method, The RF exposure has then been extrapolated by setting $F_{\mathrm{ExtBeam}} = 19$, $F_{\mathrm{BW}} = 2592$, $F_{\mathrm{TDC}} = 1$, and $F_{\mathrm{PR}} = 1$ in equation (9). The results of Fig. 7 indicate that the exposure variations (as a function of the beam angle) measured by both methods follow a reasonably similar trend, especially for the main beam at around 10 degrees. To put things into perspective, it is important to note that the E-field strength curve is based on thousands of measurements over a 48h period, while the SSB method is only based on 190 measurements (10 measurements per beam direction for each of the 19 beam directions) over a 40 min period. More SSB measurements could help with the accuracy of the method. This figure also shows the importance of the scaling factor values for correctly assessing the exposure, which in turn require field strength measurements, as in [9], for properly calibrating the results.

B. INFLUENCE OF THE NUMBER OF ACTIVE RF CHANNEL/ANTENNA ON THE RF-EMF EXPOSURE

As we already mentioned in Section II-A, the total transmit power of our mMIMO BS, P, grows linearly with the number of utilized RF channels n, such that $P = pn$, where p is the per-channel transmit power. Given that the aggregate antenna gain of the mMIMO array, G grows also linearly with the number of utilized RF channels, such that $G = gn$, where g is the per-antenna element gain, it is expected from

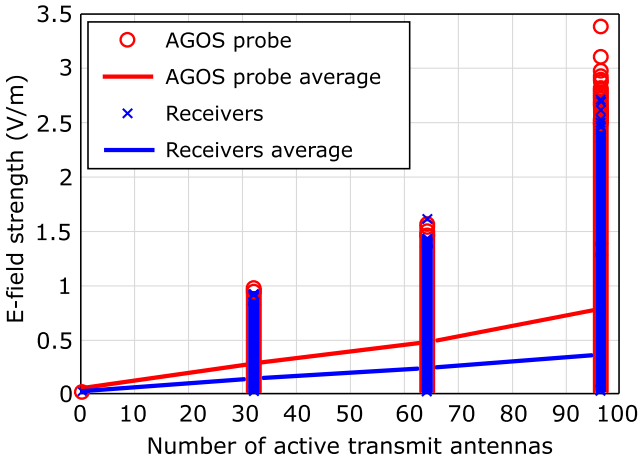

FIGURE 8. RF-EMF exposure (individual measurements and average) of the mMIMO testbed as a function of the number of active transmit antennas.

equation (4) that the exposure/E-field grows linearly with n, i.e., $E \propto \sqrt{n^2 pg}$. This can clearly be observed in Fig. 8 where the average RF-EMF exposure (in V/m), which was measured by both the probe and receivers, grows roughly linearly with the number of RF channels/antennas at the BS. Note that each blue cross or red circle in Fig. 8 represents an individual measurement acquired by the receivers or AGOS probe, respectively, and each solid line is the average of all the thousands of receivers/probe measurements.

C. INFLUENCE OF THE RELATIVE POSITION OF THE ACTIVE UEs ON THE RF-EMF EXPOSURE

Figure 9 depicts the RF-EMF measurement results acquired through the mMIMO testbed when 96 Tx antenna elements were used, and only one beam was active and steered in the direction indicated by the x-axis. In Fig. 9, each blue cross represents one exposure measurement and the red curve is the averaged exposure. More precisely, Fig. 9 depicts the results measured through the AGOS probe and antenna 1 of the five receivers, positioned as in Fig. 2, where the receivers act as extra probes. These results first clearly show that the maximum of the exposure is reached when the beam is steered in the general direction of each probe. For instance, antenna 1 of receiver 1 or receiver 2 is roughly $+5°$ or $-15°$ away from the centre of the BS array (i.e., $\arctan(0.3/3)$ or $-\arctan(1.05/4.05)$ according to Fig. 2 b)), respectively, and the results show that the maximum of the exposure is reached at roughly $+5°$ or $-15°$ for these two probes, which also confirm the accuracy of our OTA-calibration for the mMIMO system. They also indicate that the variations of the exposure can be quite significant when the beam points towards the probes or not. According to the AGOS probe exposure result in Fig. 9, a user or bystander average exposure could be up to nine times higher when a beam points towards them or not, when located at the AGOS probe position, i.e., at the coordinate (1.05 m, 3 m) of Fig. 2 b) grid. Indeed, the maximum of the average exposure measured by the AGOS probe in Fig. 9, which occurs when the beam is steered towards the

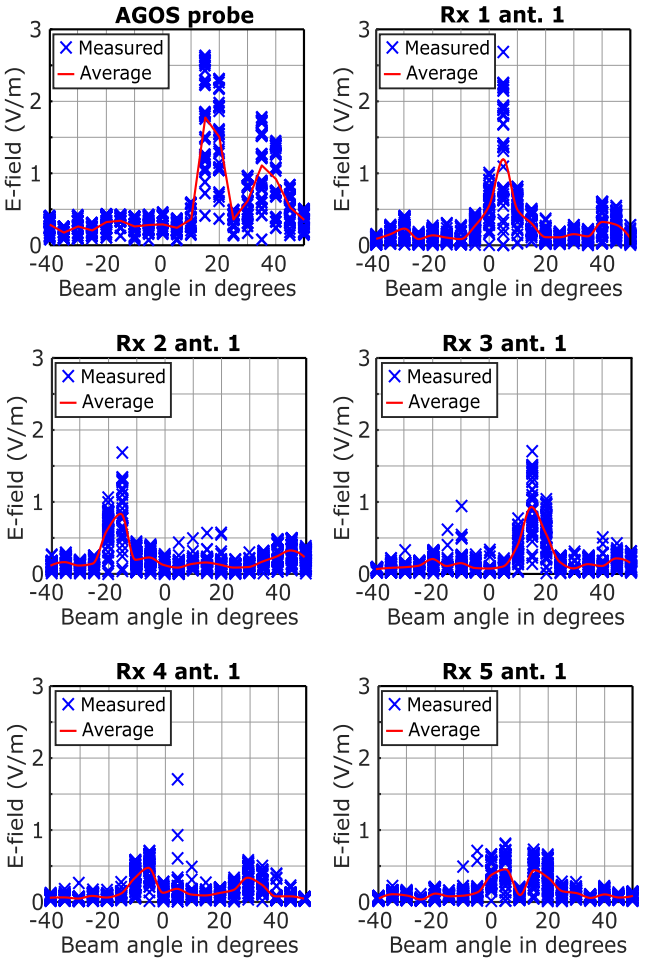

FIGURE 9. RF-EMF exposure of the mMIMO testbed measured at the probe and antenna 1 of the five receivers as a function of the beam angle when only one beam is active at the mMIMO BS and steered from $-40°$ to $50°$ in azimuth relative to the centre of the mMIMO array.

probe (i.e. at a beam angle of roughly $+15°$) is approximately 1.8 V/m. Whereas the minimum of the average exposure is approximately 0.2 V/m, at a beam angle of roughly $-35°$, such that the ratio between the maximum and minimum exposure values is nine (i.e., 1.8/0.2). While the maximum of the exposure occurs when the beam is steered towards the probe, the minimum/floor of the exposure is mainly due to the side lobes of the beam. Finally, as it is expected from equations (5) and (6), the exposure is inversely proportional to the distance; the maximum amplitude of the exposure at antenna 1 of Rx 5 (i.e., 7 m away from the BS) is at least two times lower than the one at antenna 1 of Rx 1 (i.e., 3 m away from the BS).

Figure 10 shows the empirical RF-EMF exposure measurement results of the commercial 5G BS in a similar setup as in Fig. 9, i.e., when only one of the UE terminal is active at a time and different transmission data rates are considered. In addition, as in Fig. 9, the RF-EMF exposure was measured when the BS was not necessarily transmitting towards the AGOS probe, i.e., the probe acted as a bystander. The results of Fig. 10 confirm, as in Fig. 9, that the relative position

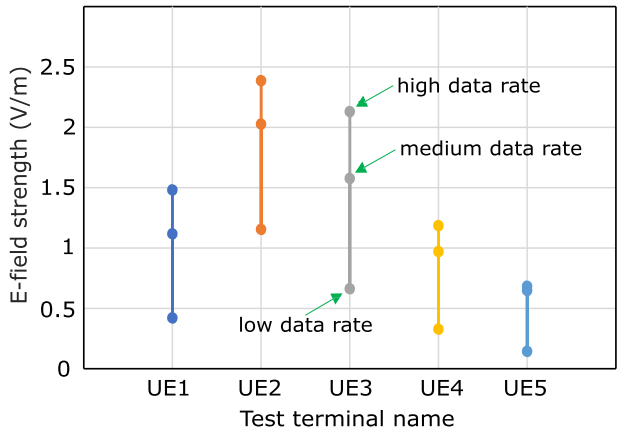

FIGURE 10. RF-EMF exposure results of UE1 to UE5 in different traffic loads when only one of the UE terminal is active at a time, based on the commercial 5G BS measurements.

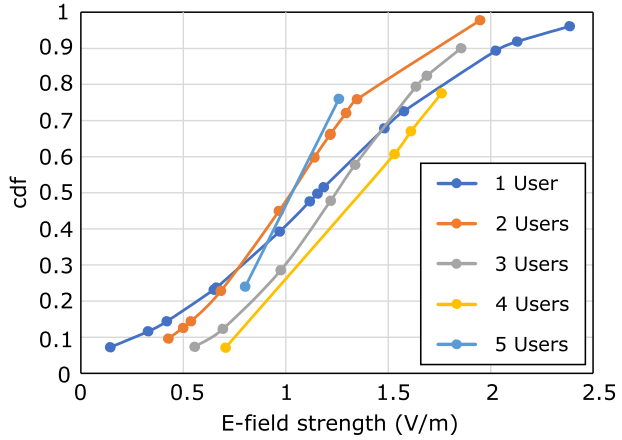

FIGURE 11. Cdf of the RF-EMF exposure for various numbers of active UEs, based on the commercial 5G BS measurements.

of the active UEs towards the measurement location has a significant impact on the measured exposure, with higher levels reached when the active UE is closer to the probe, i.e., near UE2. In addition, as in Fig. 9, significant exposure variations can be noticed depending on the beam direction. For instance, the maximum exposure measured by the probe when the BS transmits to UE2 is roughly 3.5 times higher than when it transmits to UE5. A similar observation was made in [14], where it is stated that the exposure depends on the duration of presence of the beam in a given direction.

D. INFLUENCE OF THE NUMBER OF ACTIVE UEs ON THE RF-EMF EXPOSURE

Figure 11 illustrates the statistical variations of the RF-EMF exposure as a function of the number of active UEs based on the commercial 5G BS measurements. More specifically, it shows how the cumulative distribution function (cdf) of the exposure differs for different numbers of users when the amount of traffic remains similar regardless of the number of active UEs. The results show that the variance of the exposure tends to decrease as the number of users increases, or in other words, the main slope of each cdf curve gets steeper as the number of users increases. This trend is visible when

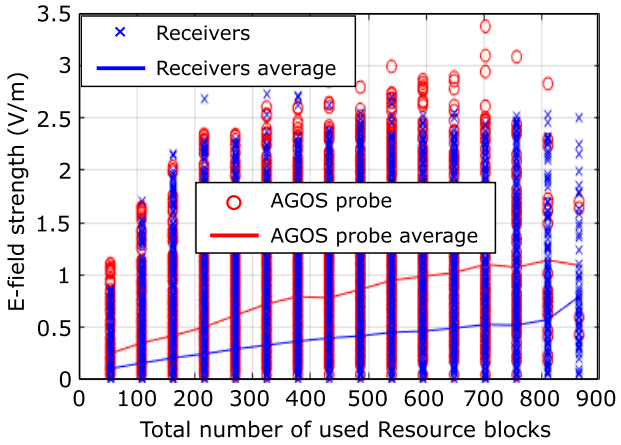

FIGURE 12. RF-EMF exposure (individual measurements and average) of the mMIMO testbed as a function of the number of used resource blocks.

jointly analyzing the results for "1 User", "3 Users", and "5 Users". It can also be remarked in Fig. 11 that the median (50th percentile) value of the exposure is quite similar for some configurations (i.e. "2 Users" and "5 Users") while the range of possible exposure values is reduced. It turns out that this result is in line with the theoretical study of [7], where it is explained and showed in Figures 4 to 7 of [7] that the variance of the aggregate antenna gain as well as total transmit power and, hence, the variance of the exposure (based on equations (4) and (6)) decreases as the number of users increases, while the median value of both these quantities remains similar.

E. INFLUENCE OF THE TRAFFIC PATTERN OF THE ACTIVE UEs ON THE RF-EMF EXPOSURE

Figure 12 depicts the variations of the exposure as a function of the number of utilized RBs based on the mMIMO testbed measurements, where each blue cross or red circle represents one measurement, and each solid line is the average of these measurements. The averaged results for both the probe and receivers suggest that the average RF-EMF exposure (in V/m) grows sub-linearly with the number of used RBs. The higher the number of used RBs, the higher the data rate, but the higher the required transmit power. Given that the E-field is proportional to the square root of the transmit power (see equations (4) and (6)), it is expected that the E-field strength should grow proportionally with the square root of the number of used RBs, which is somehow the trend in Fig. 8 c). This finding also validates the use of the factor $\sqrt{F_{\mathrm{BW}}}$ in equations (8) and (9) to scale the exposure in the SSB method, since it is related to the number of utilized RBs.

The results of Fig. 10 for the commercial 5G BS confirms that the exposure varies as a function of the active UE traffic pattern, with the highest level of exposure measured when the active UE(s) request(s) the maximum data rate of 700 Mbps. It is also clear from Fig. 10 that the increase in exposure between low to medium and medium to high data rates is sub-linear, i.e., the increase is larger between low to medium than between medium to high data rates.

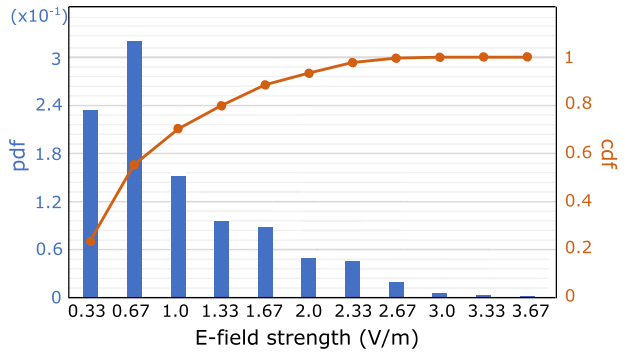

FIGURE 13. Pdf and cdf of the RF-EMF exposure based on all the mMIMO testbed measurements.

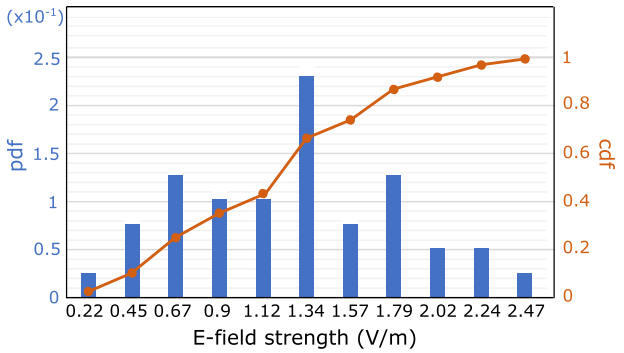

FIGURE 14. Pdf and cdf of the RF-EMF exposure based on all the commercial 5G BS measurements.

F. INFLUENCE OF THE ENVIRONMENT ON THE RF-EMF EXPOSURE

Even though the measurement results of Fig. 9 were obtained for only one active beam, this figure indicates that more than one beams are detected by most of the probes, i.e. the RF-EMF exposure peaks at more than one transmitted angle. The main peak is caused by the direct LoS propagation path between the mMIMO Tx and each probe, while the second peak is likely caused by an indirect propagation path reflecting off an object in close proximity, most probably the window and/or its frame on the side of the experiment.

Whereas in Fig. 10, it is expected that the level of exposure around the probe should be higher when beams are pointed towards its location and lower otherwise. The results for UE2, UE3, UE4, and UE5 in Fig. 10 are in line with this expectation, given that the distance between the probe and each of these UEs follows the same ascending ordering. However, the exposure for UE3 is higher than that of UE1, even though UE1 is closer from the probe than UE3. This is likely due to the fact that, contrary to UE3 that is in LoS with the 5G BS, the LoS path from the 5G BS to UE1 is partially blocked by a leaning tree, as it can be seen in Fig. 4 b).

These two examples of environmental effects on the RF-EMF exposure of 5G BS reinforces its statistical nature.

G. DEFINING THE BS EXCLUSION ZONE BASED ON STATISTICAL RF-EMF EXPOSURE

The statistical nature of the exposure has obviously an impact on the definition of BS exclusion boundary. For instance, it was suggested in [7] that the exposure value corresponding to the 99-th or 95-th percentile of the exposure cdf should be used for defining the exclusion zone of 5G BS instead of defining it based on the maximum EIRP. This can reduce the radius of the exclusion boundary, a.k.a. compliance distance, by nearly half, according to [7].

Figure 13 and 14 outline the normalized probability distribution function (pdf) and cdf of the RF-EMF exposure generated by the mMIMO testbed and commercial 5G BS, respectively, based on all the E-field data collected by the probe(s) for various UE configurations, e.g., various numbers of active users/beams, various levels of targeted data rates for each users. For the 5G BS measurement campaign, 17 different configurations of active UEs/targeted data rates were used for gathering data, e.g., a single UE active at a time with a data rate of 700 Mbps, two active users with a target data rate of 350, 230, or 35 Mbps, or five active users with a target data rate of 120 or 30 Mbps. The results indicate that the shape of each pdf/cdf is rather different in both cases. This difference can be due to the beamforming implementation, which is unlikely to be the same for both BSs, the amount of data collected (i.e., the mMIMO testbed collected far more data than the commercial 5G BS), or the type of data (i.e., instantaneous instead of 6 min average exposure).

In Fig. 13, the mode, i.e., the most frequent value of the pdf, of the exposure is 0.67 V/m, the average exposure is around 0.98 V/m and the maximum measured exposure is 3.67 V/m. Assuming that the 95th percentile of the cdf occurs at an exposure of 2.33 V/m, based on Fig. 13, and that the probe was placed 3.18 m away from the centre of the mMIMO BS array, this exposure value corresponds to an EIRP of 32.6 dBm based on equations (4) and (6). In turn, this EIRP corresponds to a compliance distance of 0.12 m, when the maximum exposure limit is based on the ICNIRP value of 61 V/m. Whereas the compliance distance is equal to 0.28 m for the maximum EIRP of 40 dBm and the 61 V/m limit. Hence, the compliance distance could be reduced by around 52% based on the 95th percentile. In Fig. 14, the mode of the exposure is 1.34 V/m, the average exposure is around 1.27 V/m and the maximum measured exposure is 2.47 V/m. Assuming that the 95th percentile of the cdf occurs at an exposure of 2.36 V/m, based on Fig. 14, and that the probe was placed 162.32 m away from the 5G BS, this exposure value corresponds to an EIRP of 66.9 dBm based on equations (4) and (6). In turn, this EIRP corresponds to a compliance distance of 6.28 m for the 61 V/m exposure limit. Whereas the compliance distance is equal to 10.07 m for the maximum EIRP of 71 dBm and the 61 V/m limit. Hence, the compliance distance could be reduced by around 38% based on the 95th percentile. Overall, these results are in line with the work of [7].

It is also important to bear in mind that the ICNIRP value is not used in every country in the world and some countries like for instance Italy, Belgium, or Bulgaria have more stringent limits, e.g., 6 V/m (Italy attention value, Bulgaria general

limit). Based on the maximum EIRP rule, the compliance distance would be 102.42 m for the 5G commercial BS with an exposure limit of 6 V/m, such that more than half of the test area in Fig. 3 would be off-limit. Whereas, for an EIRP of 66.9 dBm (corresponding to the 95th percentile of the cdf of Fig. 14), the compliance distance would still be large enough, i.e., 63.88 m, to severely restrict the deployment of the 5G BS. Hence, lower percentile could be envisaged for defining the compliance distance of 5G BS in countries with stringent exposure limits, especially if the pdf of the exposure is closer to a Gaussian than a Poisson distribution, as in Fig. 13.

V. CONCLUSION

This paper has studied the stochastic nature of the EMF exposure and how it can impact the definition of the exclusion boundary, especially under the constraint of stringent exposure limits, by relying on two different approaches for gathering experimental-based evidences. First we have used a fully reconfigurable mMIMO testbed for evaluating the spatial and temporal variations of the RF-EMF exposure in a controlled outdoor scenario. Then, we have used a typical commercial 5G BS to complement/confirm some of the results/trends obtained via the mMIMO testbed. Several important insights can be inferred from our measurement campaign results:

- EMF exposure due to 5G BS grows linearly with the number of utilized RF chains at the BS.
- Significant exposure variations can result from the beam directionality, i.e. the relative position of the exposure measurement location to the beam direction has a significant impact on the measured exposure. This suggests a very dynamic/changing exposure environment driven by active UEs in 5G, in clear contrast with previous cellular technologies.
- Environmental effects, such as indirect propagation paths (e.g. reflecting off objects) or blocked paths can also create further variations.
- The variance of the exposure tend to decrease as the number of active UEs increases when the traffic remains constant, or in other words it becomes more deterministic. Whereas the exposure grows sub-linearly with the traffic, regardless of the number of active UEs.
- The statistical distribution of EMF exposure for 5G BSs should be better understood and probably taken into account for defining the exclusion boundary. The results of our two measurement campaigns indicate that the statistics of different 5G BSs are not necessarily the same, i.e., the exposure of our mMIMO testbed BS follows a Poisson distribution while the commercial 5G BS exposure is closer to a normal distribution. In turn, this can impact the exclusion boundary size when it is defined as a particular percentile of the exposure cdf.
- Defining the BS exclusion boundary based on the 95-th percentile seems to not be a flexible enough approach to accommodate the deployment of 5G BS in countries/places with stringent EMF exposure limits. Our measurement results correspond to a boundary size in the order of several tens of meters for an exposure limit of 6 V/m based on the 95-th percentile.
- The quality and quantity of field strength data collection need to be carefully considered to properly tune the extrapolation parameters in the SSB method as well as to accurately model the EMF exposure distribution of a particular 5G BS site.

In the future, we would like to extend this work to mm-wave frequencies and build a empirical statistical model of the EMF exposure based on the same metrology approach.

ACKNOWLEDGMENT

The authors would like to acknowledge the support of the University of Surrey 5GIC and 6GIC (http://www.surrey.ac.uk/5gic) members.

REFERENCES

[1] A. Tölli, L. Thiele, S. Suyama, G. Fodor, N. Rajatheva, E. De Carvalho, W. Zirwas, J. H. Sorensen, M. Dohler, and T. Nakamura, "Massive multiple-input multiple-output (MIMO) systems," in *5G Mobile and Wireless Communications Technology*, A. Osseiran, J. F. Monserrat, and P. Marsch, Eds. Cambridge, U.K.: Cambridge Univ. Press, Jun. 2016, ch. 8, pp. 208–247.

[2] M. A. Jamshed, F. Heliot, and T. W. C. Brown, "A survey on electromagnetic risk assessment and evaluation mechanism for future wireless communication systems," *IEEE J. Electromagn., RF Microw. Med. Biol.*, vol. 4, no. 1, pp. 24–36, Mar. 2020.

[3] L. Chiaraviglio, A. S. Cacciapuoti, G. Di Martino, M. Fiore, M. Montesano, D. Trucchi, and N. B. Melazzi, "Planning 5G networks under EMF constraints: State of the art and vision," *IEEE Access*, vol. 6, pp. 51021–51037, 2018.

[4] R. Pawlak, P. Krawiec, and J. Z. urek, "On measuring electromagnetic fields in 5g technology," *IEEE Access*, vol. 7, pp. 29826–29835, 2019.

[5] *Determination of RF Field Strength, Power Density and SAR in the Vicinity of Radiocommunication Base Stations for the Purpose of Evaluating Human Exposure*, International Electrotechnical Commission (IEC), Geneva, Switzerland, Standard IEC TR 62232, Aug. 2017. [Online]. Available: https://webstore.iec.ch/publication/28673

[6] B. Thors, A. Furuskär, D. Colombi, and C. Törnevik, "Time-averaged realistic maximum power levels for the assessment of radio frequency exposure for 5G radio base stations using massive MIMO," *IEEE Access*, vol. 5, pp. 19711–19719, 2017.

[7] P. Baracca, A. Weber, T. Wild, and C. Grangeat, "A statistical approach for RF exposure compliance boundary assessment in massive MIMO systems," in *Proc. 22nd Int. ITG Workshop Smart Antennas (WSA)*, Bochum, Germany, Mar. 2018, pp. 1–6.

[8] *Case Studies Supporting IEC 62232—Determination of RF Field Strength, Power Density and SAR in the Vicinity of Radiocommunication Base Stations for the Purpose of Evaluating Human Exposure*, Standard IEC TR 62669, International Electrotechnical Commission (IEC), Geneva, Switzerland, Apr. 2019. [Online]. Available: https://webstore.iec.ch/publication/62014

[9] S. Aerts, L. Verloock, M. Van Den Bossche, D. Colombi, L. Martens, C. Törnevik, and W. Joseph, "In-situ measurement methodology for the assessment of 5G nr massive MIMO base station exposure at sub-6 GHz frequencies," *IEEE Access*, vol. 7, pp. 184658–184667, 2019.

[10] F. Pythoud. (Feb. 2020). *Technical Report: Measurement Method for 5G NR Base Stations up to 6 GHz*. Federal Institute of Metrology METAS. [Online]. Available: https://www.metas.ch/metas/en/home/dok/publikationen/meldungen/2020-02-18.html

[11] G Ziegelberger, R. Croft, M. Feychting, A. C. Green, A. Hirata, G. d'Inzeo, K. Jokela, S. Loughran, C. Marino, S. Miller, and G. Oftedal, "ICNIRP guidelines for limiting exposure to electromagnetic fields(100 KHz to 300 GHz)," *Health Phys.*, vol. 118, no. 5, pp. 483–524, May 2020.

[12] (Sep. 2019). International Telecommunication Union (ITU). *The Impact of RF-EMF Exposure Limits Stricter Than the ICNIRP or IEEE Guidelines on 4G and 5G Mobile Network Deployment*. ITU, Geneva, Switzerland, ITU-T K-series Recommendations. [Online]. Available: https://www.itu.int/rec/T-REC-K.Sup14-201909-I/en

[13] (Feb. 2020). The Office of Communications (OfCom). *Electromagnetic Field (EMF) Measurements Near 5G Mobile Phone Base Stations*. [Online]. Available: https://www.ofcom.org.U.K./_data/assets/pdf_file/0015/190005/emf-test-summary.pdf
[14] (Apr. 2020). Agence Nationale des Fréquences (ANFR). *Assessment of the Exposure of the General Public to 5G Electromagnetic Waves*. AFNR. [Online]. Available: https://www.anfr.fr/fileadmin/mediatheque/documents/5G/20200410-ANFR-rapport-mesures-pilotes-5G-EN.pdf
[15] D. Colombi, P. Joshi, B. Xu, F. Ghasemifard, V. Narasaraju, and C. Törnevik, "Analysis of the actual power and EMF exposure from base stations in a commercial 5G network," *Appl. Sci.*, vol. 10, no. 15, pp. 359–5280, 2020.
[16] A.-K. Lee, S.-B. Jeon, and H.-D. Choi, "EMF levels in 5G new radio environment in Seoul, South Korea," *IEEE Access*, vol. 9, pp. 19716–19722, 2021.
[17] T. H. Loh, F. Heliot, D. Cheadle, and T. Fielder, "An assessment of the radio frequency electromagnetic field exposure from a massive MIMO 5G testbed," in *Proc. 14th Eur. Conf. Antennas Propag. (EuCAP)*, Copenhagen, Denmark, Mar. 2020, pp. 1–5.
[18] T. H. Loh, D. Cheadle, F. Heliot, A. Sunday, and M. Dieudonne, "A study of experiment-based radio frequency electromagnetic field exposure evidence on stochastic nature of a massive MIMO system," in *Proc. 15th Eur. Conf. Antennas Propag. (EuCAP)*, Dusseldorf, Germany, Mar. 2021, pp. 1–5.
[19] S. Yang. (Feb. 2021). *Electromagnetic Field (EMF) Triaxial Isotropic Antenna*. Keysight Technologies. [Online]. Available: https://www.keysight.com/gb/en/assets/3121-1035/data-sheets/Electromagnetic-Field-EMF-Triaxial-Isotropic-Antenna.pdf
[20] P. Muschamp, T. Ghosh, C. Williams, and A. Donohoe. (Jun. 2021). *Solution Facility Sites High Level Design (HLD)—V1 U.K. Facility Site Annex (Release 4)*. 5G-Verticals Inovation Infrastructure (VINNI). [Online]. Available: https://www.5g-vinni.eu/wp-content/uploads/2019/02/5g-vinni_d2.1_annex_a2_uk.pdf
[21] *Specification for Radio Disturbance and Immunity Measuring Apparatus and Methods—Part 1–6: Radio Disturbance and Immunity Measuring Apparatus—EMC Antenna Calibration*, Standard CISPR 16-1-6, International Electrotechnical Commission (IEC), Geneva, Switzerland, Dec. 2014. [Online]. Available: https://webstore.iec.ch/publication/62014
[22] Y. Ji, J. O. Nielsen, and W. Fan, "A simultaneous wideband calibration for digital beamforming arrays at short distances [measurements corner]," *IEEE Antennas Propag. Mag.*, vol. 63, no. 3, pp. 102–111, Jun. 2021.
[23] H. Wang and Y. Gui, "Metrology for channel sounding," in *Metrology for 5G and Emerging Wireless Technologies*, T. H. Loh, Ed. London, U.K.: The Institution of Engineering and Technology, Dec. 2021, ch. 8.
[24] D. Franci, S. Coltellacci, E. Grillo, S. Pavoncello, T. Aureli, R. Cintoli, and M. D. Migliore, "An experimental investigation on the impact of duplexing and beamforming techniques in field measurements of 5G signals," *Electronics*, vol. 9, no. 2, p. 223, Jan. 2020.

FABIEN HÉLIOT (Member, IEEE) is currently a Lecturer in wireless communications at the Institute for Communication Systems (ICS), University of Surrey. He has published more than 100 peer-reviewed papers, book chapters, and technical reports in diverse areas of communications theory and signal processing for wireless communications. He has lead the EPRSC funded project "Electromagnetic field exposure reduction/avoidance for the next generations of wireless communication systems" and has been actively involved in other funded U.K./EU projects related to the topic of this work, such as metrology for RF EXposure from 5G base station (5GRFEX) and Low Exposure Future Networks (LExNet). He received an Exemplary Reviewer Award from the IEEE COMMUNICATIONS LETTERS, in 2011, and the Best Paper Award from the EuCNC Conference, in 2011 and 2021.

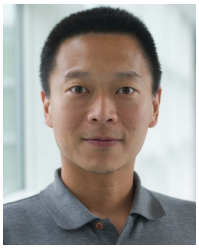

TIAN HONG LOH (Senior Member, IEEE) received the Ph.D. degree in engineering from the University of Warwick, U.K., in 2005. He has been with the National Physical Laboratory (NPL), U.K., since 2005. He is currently a Principal Research Scientist at NPL. He leads work at NPL on a wide range of applied and computational electromagnetic metrology research areas to support the telecommunications industry. He is also a Visiting Professor at the University of Surrey, U.K., a Visiting Industrial Fellow at the University of Cambridge, U.K., and a U.K. Representative of URSI Commission A (Electromagnetic Metrology). He holds six patents, one book, and nine book chapters. He has authored and coauthored over 180 refereed publications. His research interests include 5G communications, smart antennas, small antennas, metamaterials, body-centric communications, wireless sensor networks, electromagnetic compatibility, and computational electromagnetics.

DAVID CHEADLE was born in London, U.K. He is currently pursuing the B.Eng. degree in electrical and electronic engineering with London South Bank University. He joined the National Physical Laboratory, Teddington, U.K., as an Assistant Research Scientist, in 2006, and has been promoted to a Research Scientist and a Higher Research Scientist, in 2011 and 2018, respectively. He has over ten years of experience in EMC and antenna metrology. He has been involved in providing measurement services in support of the electronics and communication industry. He currently holds 21 publications. He currently works with the Electromagnetic Technologies Group on research projects related to the measurement of beamforming antennas, fifth-generation and future communication systems, and establishment of wireless communication testbeds using software-defined-radios.

YUNSONG GUI received the bachelor's degree in electronic information engineering from Nanchang University, China, in 2002, and the master's degree in electromagnetic filed and microwave from Shanghai Jiao Tong University, China, in 2006. He has worked as a Senior Baseband and a RF Engineer at Huawei and a Senior Researcher at the Chinese Academy of Sciences. In 2020, he joined the National Physical Laboratory (NPL), Teddington, U.K., as a Senior Research Scientist. He has over 15 years of experience in wireless communication and RF system design and performance verification. His current research interests include wireless channel modeling, and verification and SDR-based wireless testbeds.

MICHAEL DIEUDONNE is currently the Director of Keysight Technologies Belgium BV (Keysight BE), Rotselaar, Belgium. He is also a Department Manager at Keysight Labs and supervises research performed in different domain around 5G/6G, network test, and high frequency metrology. He has been active in various international project, such as the EURAMET EMPIR MET5G Project, the EU SAMURAI Project defining early day MIMO techniques for 4G systems, and coordinated EU-H2020 Triangle (test of application in a 5G context). Today he works on 5G-VINNI 5G networking test, SIP 5GRFEX for 5G EMF measurements, and other internal programs.